PAPER

Check for updates

A self-powered droplet sensor based on a triboelectric nanogenerator toward the concentration of green tea polyphenols†

Guochen Lin,[a,b] Chang Su,[a,b] Chengmin Bao,[a,b] Maoyi Zhang,[a] Chuanbo Li*[b] and Ya Yang [ID] *[a,c]

Self-powered liquid droplet sensors based on triboelectric nanogenerators have attracted extensive attention in the field of biochemical sensing applications. Numerous research studies have investigated the effects of factors such as molecular species, molecular concentration, molecular charge, and molecular dipole moment in solution on the output electrical signals of the sensor. In this study, we prepared a self-powered droplet sensor using conductive copper film tape, polytetrafluoroethylene, and conductive aluminum foil tape. The sensor can continuously output pulsed electrical signals with minimal environmental impact. In comparison with other types of sensors, this sensor boasts a rapid response time of 10 ms and excellent sensitivity. The relationship between the friction-induced output current and voltage of the droplets and the concentration of green tea polyphenols (GTPs) was studied using the self-powered liquid droplet sensor with five different green tea samples. It was found that GTPs were the main factor contributing to the changes in output electrical signals in green tea water droplets. Fluorescence spectroscopy was used to reveal that the magnitude of the output current was inversely proportional to the concentration of GTPs in green tea. These results demonstrate the potential application of self-powered liquid droplet sensors in biochemical sensing applications based on concentration-dependent output signals.

Introduction

In 2012, Wang and his colleagues first proposed a self-powered solid–solid triboelectric nanogenerator (TENG),[1] which was a novel power generation device based on contact electrification and electrostatic induction. Merging the energy of friction and electricity, this generator boasts self-sufficiency, eliminating the need for external power sources. The TENG holds great promise in the field of new energy with portability,[2–5] high efficiency,[6–9] and remarkable longevity.[10–12]

Subsequently, Wang and his team expanded the energy harvesting capabilities of the self-powered friction-based nanogenerator from solid–solid interactions to include liquid–solid friction in 2013.[13] They introduced Wang's hybrid model and elucidated the "two-step" formation process of the electric double layer (EDL),[14] providing an explanatory framework for the underlying mechanism behind the generation of electricity through liquid–solid friction. The structure of the self-powered liquid–solid triboelectric nanogenerator device primarily comprises the conductive electrodes, the hydrophobic polymer friction layer, and the liquid droplet friction layer. Additionally, there is a substrate that provides structural support for the device. These elements synergistically enable the efficient generation of electricity through the fascinating phenomenon of liquid–solid friction. The conductive electrodes are typically made of cost-effective metals such as copper foil or aluminum foil. They play a vital role in the generation of output current signals through the principles of electrostatic induction and potential difference. The friction layer is composed of a polymer with high electronegativity and exceptional hydrophobic properties. Examples of such polymers include PVDF (polyvinylidene fluoride),[15] FEP (fluorinated ethylene propylene),[16] PTFE (polytetrafluoroethylene),[17] nylon,[18] Kapton,[19] and so on. This friction layer enhances electron transfer and ion adsorption upon contact with the liquid droplet. When the liquid droplet diffuses, it simultaneously interacts with the friction layer and the conductive electrodes, creating a closed circuit structure. This facilitates the conversion of energy from

[a]*Beijing Key Laboratory of Micro-Nano Energy and Sensor, Center for High-Entropy Energy and Systems, Beijing Institute of Nanoenergy and Nanosystems, Chinese Academy of Sciences, Beijing 101400, P. R. China. E-mail: yayang@binn.cas.cn*
[b]*College of Life and Environmental Science, Minzu University of China, Beijing 100081, P. R. China*
[c]*School of Nanoscience and Technology, University of Chinese Academy of Sciences, Beijing 100049, P. R. China*
†Electronic supplementary information (ESI) available. See DOI: https://doi.org/10.1039/d4nr01799d

the liquid droplet into electrical energy, resulting in the generation of output electrical signals. The types of particles, particle concentration, temperature, humidity, and other factors in a solution can generate different output electrical signals. Based on these unique signals, various self-powered liquid–solid sensors have been successfully developed, leading to groundbreaking applications in the field of biochemistry sensing. Zhang and colleagues developed a droplet-TENG that showed high sensitivity to the ratio of solvents in a mixed organic solution and their work demonstrated chemical sensing applications based on the self-powered droplet triboelectric nanogenerator.[20] Later, Zhang and colleagues introduced the methodology of triboelectric spectroscopy (TES), which can detect over 30 types of common salts, acids, bases and organic molecules. The qualitative and quantitative accuracy of the TES methodology is close to 93%, and the detection limit is as low as ppb levels.[21] Wang and his colleagues have pioneered a specific bacterial biosensor based on a single-droplet triboelectric nanogenerator. This remarkable innovation allows for the sensitive and selective detection of *Pseudomonas aeruginosa*, with a low detection limit of 4.5×10^3 CFU mL^{-1}.[22] Li and colleagues have pioneered a novel temperature sensor, which is based on a liquid–solid triboelectric nanogenerator consisting of polycaprolactone (PCL)-coated aluminum oxide. This ingenious design allows for the precise measurement of temperature changes from 20 °C to 40 °C.[23] Chatterjee and team introduced an exceptional self-powered triboelectric nanosensor (TENG) utilizing an array of TiO$_2$ nanoplates as the solid friction material. They demonstrated the nanosensor's ability to detect catechins at concentrations ranging from 100 nM to 100 μM with an impressively low detection limit of 30 nM.[24] Wei and colleagues proposed an innovative frictional electrochemical taste sensing system based on droplets that integrates deep learning data analysis.[25]

Herein, we present a two-electrode self-powered droplet sensor based on a triboelectric nanogenerator toward the concentration of green tea polyphenols (GTPs). We utilized FEP, known for its strong electronegativity and hydrophobic properties, to create the friction layer. For the electrode configuration, we opted for cost-effective copper foil tape as the bottom electrode and aluminum foil tape as the top electrode. The droplet used in our experiments was from green tea water rich in GTPs. We employed the self-powered droplet sensor to analyze the friction signal of green tea water infused with tea leaves sourced from five different locations. The resulting current values reached the microampere range, while the voltage values reached tens of volts. The output signal exhibited a rapid response time of less than 10 ms. Our experimental findings demonstrated that GTPs significantly influenced the output electrical signals generated in green tea water. Furthermore, the output electrical signals were found to be inversely proportional to the concentration of GTPs. The self-powered droplet sensor used to analyze the friction signal of the sourced droplet from green tea water infused with tea leaves exhibited a detection limit of μg mL^{-1} when measuring

the tea polyphenol content. Overall, our triboelectric nanogenerator-based self-powered droplet sensor showcased several advantageous features including fast response, high sensitivity, low cost, energy efficiency, environmental friendliness, sustainability, and compact design. This research provides valuable insights into the field of solution composition detection sensors.

Results and discussion

Sensor structure and characterization

As per historical records, tea finds its origins in the era of Emperor Shennong in ancient China around 2700 BCE. Throughout nearly five millennia, the rich tapestry of tea culture has unfurled. After nearly 5000 years of tea culture development, tea is divided into six categories according to processing technology, growing region, picking season, and fermentation degree: green tea, oolong tea, yellow tea, white tea, and black tea.[26] Fig. 1a shows the preparation of green tea water from immersing finely ground green tea in ultrapure water. The green tea water includes an abundance of GTPs, amino acids, pectin, and so on. The molecular structural formulas of GTPs is portrayed in detail in Fig. 1a.

Amongst these constituents, GTPs reign supreme as the most nutritionally valuable substance within the tea leaves. The myriad benefits bestowed upon the human body by GTPs can be attributed to their phenolic hydroxyl groups. The presence of phenolic hydroxyl groups imparts GTPs with robust antioxidant and physiological activities, rendering them potent scavengers of free radicals within the human body.[27] The remarkable effects of GTPs encompass anti-aging, anti-metal toxicity, anti-inflammatory, and anti-obesity properties. Furthermore, they demonstrate significant efficacy in preventing cardiovascular diseases, Alzheimer's disease, and age-related dementia, as depicted in detail in Fig. 1b. Hence, the content of GTPs serves as a physiological biomarker for evaluating tea quality.

The structural diagram of the self-powered droplet sensor based on friction-powered nanogenerators is depicted in Fig. 1c. The substrate is a piece of 5 cm × 5 cm × 30 μm acrylic plate, primarily serving in a supportive role. The bottom electrode comprises a piece of 5 cm × 5 cm × 30 μm conductive copper foil tape completely covering the substrate. The polymer friction layer consists of a piece of 5 cm × 5 cm × 30 μm fluorinated ethylene propylene (FEP) thin film tape facilitating electron transfer and ion adsorption upon contact with the green tea water droplet. The top electrode is crafted from a piece of 1 cm × 2 mm × 30 μm aluminum foil tape. It forms a potential difference with the bottom electrode, generating valued electrical signals.

Currently, the main methods for determining the content of GTPs in green tea water include titration,[28] near-infrared absorption spectroscopy,[29] UV-visible fluorescence spectrophotometry,[30] and chemical sensors.[31] Fig. 1d presents a comparison of the self-powered droplet sensor based on triboelectric
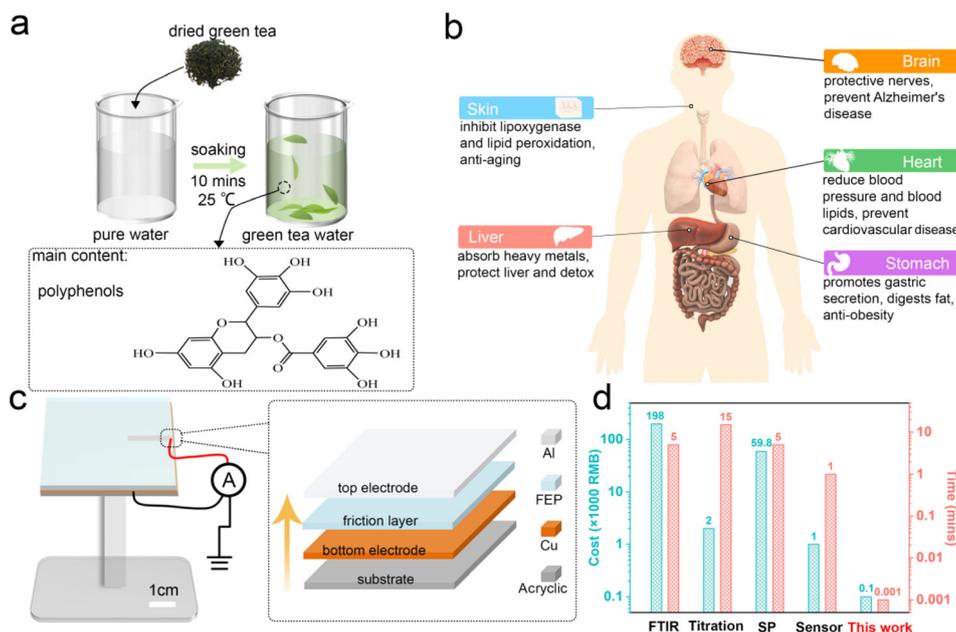
Fig. 1 (a) Preparation of green tea water. The molecular structural formula of GTPs is shown at the bottom. (b) Benefits of GTPs to the human body. (c) Schematic diagram of the layered self-powered droplet sensor. (d) Comparison of the self-powered droplet sensor with FTIR, titration, SP, and sensor in terms of cost and time consumption.

nanogenerators with the aforementioned methods in terms of cost and time consumption. The results indicate that the self-powered droplet sensor exhibits rapid response, low cost, and compact design. It thereby offers novel and significant insights into the field of solution component content detection.

The working principle of the sensor

The working principle of the self-powered droplet sensor is as follows: when the green tea water droplet comes into contact with both the FEP and aluminum foil tapes, the ions within the droplet induce the flow of charge between the electrodes, generating an electrical signal. Once the droplet departs the sensor surface, the charge flow ceases, and the electrical signal is discontinued. Fig. 2a illustrates the process of obtaining green tea water. To commence, 10 mg of finely ground Zhangjiajie green tea was carefully weighed and placed into a glass cup. Subsequently, 50 mL of pure water was added to the cup. The mixture was allowed to steep for 10 minutes at a comfortable room temperature of 25 °C. Afterward, the solution was filtered to remove any insoluble impurities, thereby obtaining the desired infusion of green tea. Fig. 2b illustrates a simulation of the working process of the self-powered droplet sensor. The green tea water from the glass cup was drawn upwards to a position approximately 20 cm above the sensor through a medical infusion tube according to the principle of siphoning. Subsequently, the green tea water was allowed to descend in the form of droplets from the outlet of the infusion tube, diffusing as they descend while coming into simultaneous contact with both the FEP and aluminum foil. Following this, the sensor forms a closed circuit, resulting in a

short-circuit current as shown in Fig. 2c. The peak magnitude of the short-circuit current is approximately 10 μA. Moreover, the generation of a short-circuit current primarily involves four distinct time intervals (i–iv). These correspond to the droplet's non-contact phase with the electrode (i), contact phase with the electrode (ii), contraction phase of the droplet (iii), and departure of the droplet (iv), as depicted in Fig. 2d. Fig. 2e depicts the equivalent circuit diagram of the self-powered droplet sensor generating output current signals,[32,33] where R_d represents the resistance of the green tea water droplet, and R_L denotes the total resistance of the circuit load.

Phase i. When a droplet falls onto the FEP friction layer interface of the LS-TENG, the FEP film easily acquires electrons when rubbing against liquid droplets and accumulates a negative charge due to the principle of friction charging. When the subsequent droplets continue to fall on the FEP, the negative charge on the FEP surface attracts the positive charge in the droplets through electrostatic induction, forming a double layer at the interface of the "FEP/droplet", which can be equated to a capacitance C_1 from the point of view of the electric circuit. Also, the capacitance with the FEP/droplet double layer as the upper electrode, FEP as the dielectric, and the copper foil as the lower electrode is expressed as C_F. C_1 and C_F are connected in series. Since the droplet is not in contact with the aluminum foil, the circuit is broken and there is no movement of electrons, and so no current is generated.

Phase ii. Due to fluid dynamics, diffusion occurs when droplets collide with the FEP layer. As the droplet diffuses, the area gradually increases, which increases the contact with the
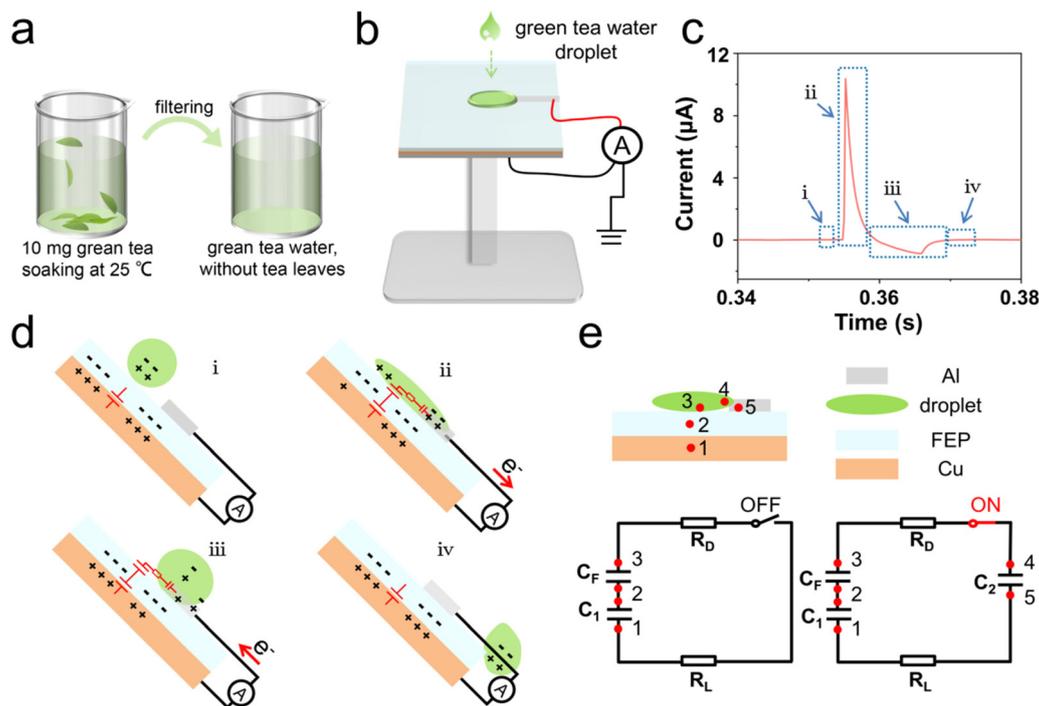
Fig. 2 (a) Process of filtering green tea water. (b) Schematic diagram of the testing process. (c) Output current signals of the sensor. (d) Working mechanism of the sensor. (e) Equivalent circuit diagram of the sensor.

aluminum electrode, and a double layer capacitance C_2 is formed on the "droplet/Al" surface. A double layer capacitance C_2 is formed on the surface of the "droplet/Al" according to the relationship between capacitance, voltage and charge of a flat capacitor as shown by the flat capacitance equation:

$$C = (\varepsilon \times A)/d \tag{1}$$

$$U = Q/C \tag{2}$$

where C is the capacitance of the flat capacitor, d is the dielectric thickness of the flat capacitor, ε is the relative dielectric constant, A is the area of the flat capacitor, and U is the voltage across the capacitor. Since the thickness of the FEP is much greater than that of the "FEP/droplet" and "droplet/Al" double layers, and the dielectric constant is smaller, the capacitance of C_F in the circuit is much smaller than that of C_1 and C_2. Furthermore, the FEP carries more charge when it rubs against the droplet so that there is a potential difference between the C_F ends due to the contribution of electrostatic charge. When the droplet diffuses and comes into contact with the aluminum electrode, it results in a larger potential difference between the two ends of C_F, thereby charging C_1 and C_2. This causes positive charge to transfer from the lower electrode to the upper electrode.

Phase iii. When C_F ends the charging process for C_1 and C_2, due to the action of surface tension, the surface of the droplet tends to shrink to its smallest surface area. As the capacitance values of C_1 and C_2 decrease, the charge stored in them starts to flow back towards C_F. This causes a reverse current, where

the electric charge from the top electrode of aluminum foil flows towards the copper foil of the bottom electrode. Because the rate of droplet contraction is relatively slower than the rate of diffusion, the peak current of the reflux is small.

Phase iv. When the droplet completely shrinks, gravity will cause it to slip from the surface of the FEP. As a result, the droplet and the aluminum electrode will become disconnected, interrupting the connection between the FEP and the electrodes. Capacitors C_1 and C_2 will then charge the C_F end, leading to the disconnection of the circuit and the cessation of charge transfer, causing the current to disappear. At this point, the sensor device returns to its initial state.

Fig. 2e is a schematic diagram of capacitors C_1, C_2 and C_F formed by the self-powered droplet sensor at different interfaces. A double electric layer capacitor C_1 is formed at the interface of the droplet (position 3) and FEP (position 2), and a double electric layer capacitor C_2 is formed at the interface of the droplet (position 4) and aluminum electrode (position 5). A capacitor C_F is formed with a double layer capacitor C_1 as the upper electrode, FEP as the dielectric (position 2), and a copper foil (position 1) as the lower electrode. The lower left diagram in Fig. 2e shows the equivalent circuit diagram of the sensor in the non-operational stage i and stage iv. When the droplet is disconnected from the aluminum electrode there is no charging between C_F, C_1 and C_2. The lower right diagram in Fig. 2e shows the equivalent circuit diagram of the sensor in the working phase ii (C_F charges C_1 and C_2) and phase iii (C_1 and C_2 charge C_F). R_d is the resistance of the droplet, and R_L is the total resistance of the circuit load.

Output signals through different solutions by the sensor

Fig. 3a shows the friction electrical output of green tea water with different solid–liquid ratios. As the solid–liquid ratio increased from 0.2 mg mL^{-1} to 1.6 mg mL^{-1}, the average short-circuit current of the Biluochun green tea water decreased from 12.14 μA to 3.59 μA (Zhangjiajie green tea decreased from 10.53 μA to 1.01 μA, Nanjian decreased from 11.84 μA to 0.89 μA, Chuluoqing decreased from 11.88 μA to 2.49 μA, and Longjing decreased from 11.14 μA to 1.17 μA). Similarly, the average open-circuit voltage of the Biluochun green tea water decreased from 51.98 V to 10.71 V (the Zhangjiajie green tea decreased from 48.82 V to 3.98 V, Nanjian decreased from 50.44 V to 2.05 V, Chuluoqing decreased from 54.53 V to 6.45 V, and Longjing decreased from 48.63 V to 2.83 V). As the solid–liquid ratio increased, the output current and output voltage values of all five types of green tea water exhibited a decreasing trend. This observation aligns with the experimental results, indicating that the concentration of ions in the droplets influences the magnitude of the output current values.[23] The short-circuit current and open-circuit voltage also decreased with increasing concentration of NaCl solution, as shown in Fig. S1.† This phenomenon can be attributed to the excess ion concentration and increased adhesive properties in the solution, leading to an electrostatic shielding effect that hinders electron transport and reduces the peak value of the output current.[34]

To confirm whether the GTPs in green tea water are the primary factors responsible for the decrease in the output electrical signal *t* of tea water droplets, it is necessary to test the trend of output electrical values for soluble GTPs, L-theanine, and pectin as their concentrations increase. In the experiment, the concentration range of the solutions was set from 0.05 to 0.4 mg mL^{-1}. The results depicted in Fig. 3b show that the
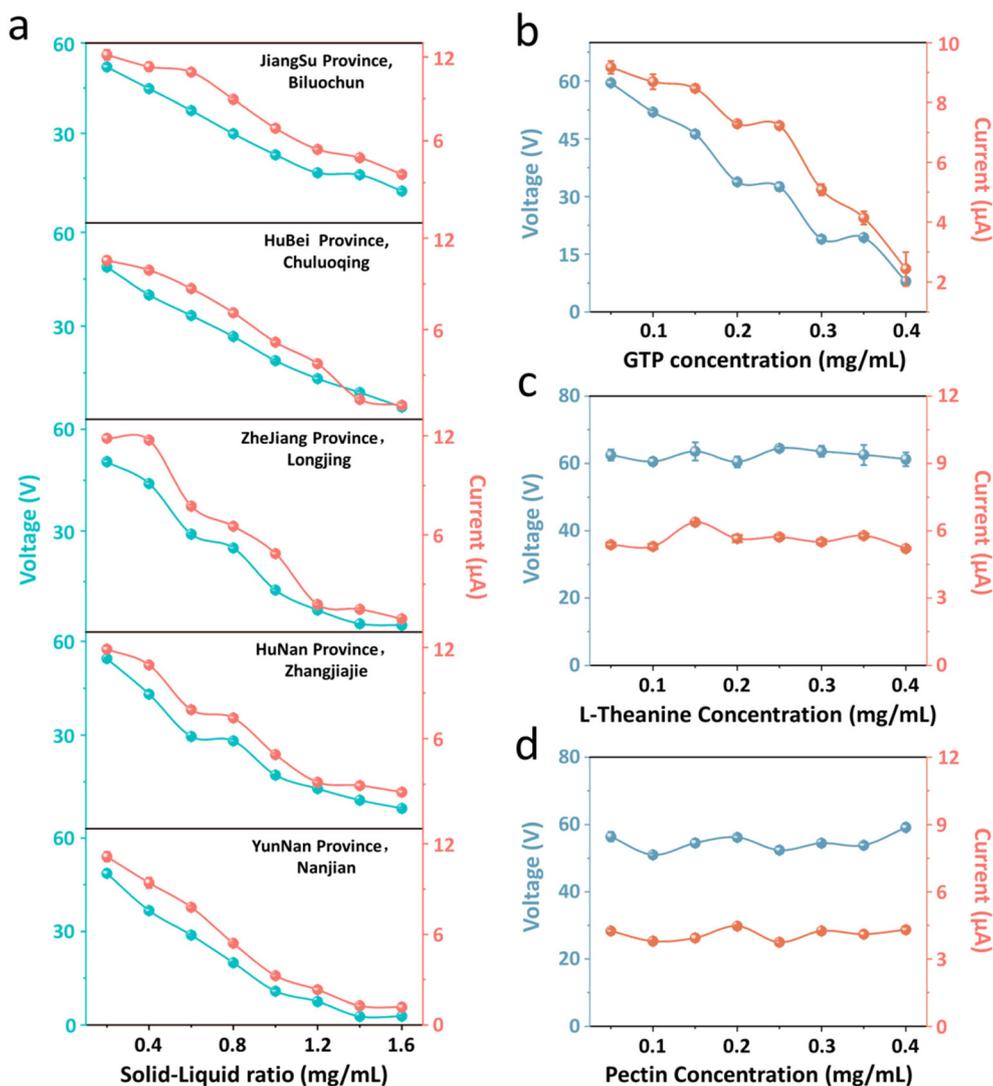

Fig. 3 (a) Output current and voltage of 5 types of green tea water with different mass ratios. (b) Output current and voltage values of GTPs with different concentrations. (c) Output current and voltage values of L-theanine. (d) Output current and voltage values of pectin.

average short-circuit current of GTP solution droplets decreased from 9.16 μA to 2.43 μA, and the average open-circuit voltage decreased from 59.47 V to 7.93 V. When the concentration of tea polyphenol solution is 0.05 mg mL^{-1}, the response time of the short-circuit current of the self-powered droplet sensor is 2 ms as shown in Fig. S2a,† and the response time of the open-circuit voltage of the sensor is 4 ms as shown in Fig. S2b.† The current sensitivity of the sensor was calculated to be from −7.99 to −40.12 μA mg mL^{-1} when the concentration of GTPs in solution increased from 0.05 mg mL^{-1} to 0.40 mg mL^{-1} as shown in Fig. S2e.† The voltage sensitivity of the sensor was calculated to be from −0.195 to −0.084 V μg mL^{-1} when the concentration of GTPs in solution increased from 50 μg mL^{-1} to 400 μg mL^{-1} as shown in Fig. S2f.† However, there was only a negligible change in both the average short-circuit current (from 5.37 μA to 5.21 μA) and average open-circuit voltage (from 62.45 V to 61.23 V) for the L-theanine solution as shown in Fig. 3c. Similarly, the pectin solution exhibited minimal variations in the average short-circuit current (from 4.25 μA to 4.31 μA) and average open-circuit voltage (from 56.44 V to 59.14 V) as shown in Fig. 3d. It can be observed that only values of GTPs decrease with increasing concentration, while the output current and voltage values of the other two components show no significantly decreasing trends. This indicates that the variation in concentration of GTPs is the main factor causing changes in the output current signals of green tea water droplets.

Application of the sensor

To validate the sensor's application in the detection of tea polyphenol concentrations, we tested the triboelectric signal and tea polyphenol concentration of green tea water from five production areas. At first, the tea polyphenol concentration of green tea water was measured by spectrophotometry using international standard methods (ISO 14502-1:2005 and ISO 14502-2:2005) and the Chinese national standard method (GB/T 8313-2018), as shown in Fig. 4a. When diluted 10 times, the absorption rates of the five green tea water working solutions are 0.261 (Biluochun), 0.272 (Chuluoqing), 0.369 (Longjing), 0.393 (Zhangjiajie), and 0.488 (Nanjian). When diluted 20 times, the absorption rates of the five green tea water working solutions are 0.125 (Biluochun), 0.129 (Chuluoqing), 0.175 (Longjing), 0.236 (Zhangjiajie), and 0.239 (Nanjian). When diluted 50 times, the absorption rates of the five green tea water working solutions are 0.041 (Biluochun), 0.043 (Chuluoqing), 0.035 (Longjing), 0.133 (Zhangjiajie), and 095 (Nanjian). Based on the absorbance values, we can calculate the concentration of GTPs in the original green tea water using the formula:

$$C(\text{mg mL}^{-1}) = \frac{A - A_0 \times V \times d \times 100}{k \times w \times 10^6 \times V_1} \quad (3)$$

Here, A is the absorption value of the green tea water working solution at 765 nm. A_0 (−0.023) is the absorption value of the ultrapure water working solution at 765 nm, V (1 mL) is the
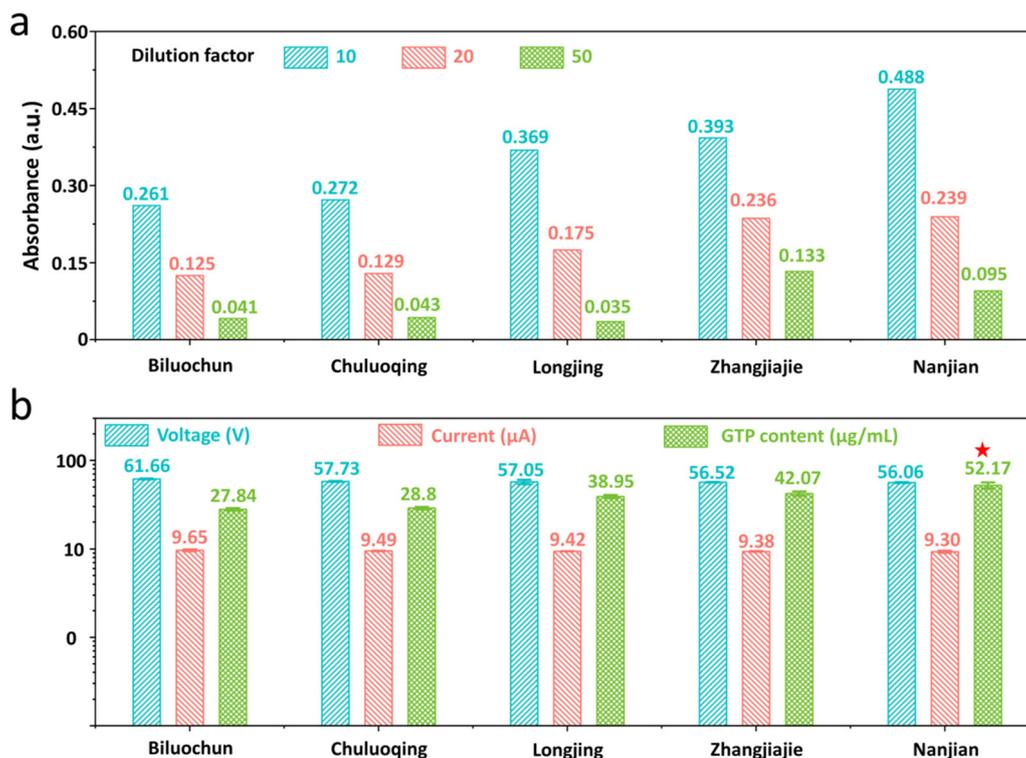

Fig. 4 (a) Absorption values of GTPs at 765 nm. (b) Output current values, output voltage values, and GTP concentrations of 5 types of GTPs at the dilution ratio of 1 : 10.

extraction volume of the green tea water, d (10, 20 and 50) is the dilution factor, k (0.01038) is the slope of the gallic acid standard curve, as shown in Fig. S3,† w (0.2 mg) is the initial mass of green tea leaves, and V_1 (50 mL) is the volume of green tea water. The average concentrations of GTPs in the initial green tea water were 0.278 mg mL^{-1} (Biluochun), 0.288 mg mL^{-1} (Chuluoqing), 0.390 mg mL^{-1} (Longjing), 0.421 mg mL^{-1} (Zhangjiajie), and 0.522 mg mL^{-1} (Nanjian). Fig. 4b shows the short circuit current, open circuit voltage and tea polyphenol concentration of green tea water from five production areas after a dilution of 10 times. The concentrations of GTPs in the green tea water from lowest to highest are as follows: Biluochun (27.84 μg mL^{-1}), Chuluoqing (28.8 μg mL^{-1}), Longjing (38.95 μg mL^{-1}), Zhangjiajie green tea (42.07 μg mL^{-1}), and Nanjian (52.17 μg mL^{-1}). The short-circuit current values from highest to lowest are as follows: Biluochun (9.65 μA), Chuluoqing (9.49 μA), Longjing (9.42 μA), Zhangjiajie green tea (9.38 μA), and Nanjian (9.30 μA). The open circuit voltage values from highest to lowest were as follows: Biluochun (61.66 V), Chuluoqing (57.73 V), Longjing (57.05 V), Zhangjiajie green tea (56.52 V), and Nanjian (56.06 V). It can be observed that the green tea water of Biluochun with the lowest content of GTPs, exhibited the highest current signal, while the Nanjian tea water showed the opposite trend. This confirms that as the concentration of GTPs increases in green tea water, the current and voltage signals of the droplets decrease. The average short-circuit current decreased from 11.26 ± 0.29 μA to 11.18 ± 0.35 μA, indicating that the device has good stability within 7 days as shown in Fig. S4.†

Conclusion

In conclusion, the self-powered droplet sensor based on triboelectric nanogenerators achieved the indirect detection of tea polyphenol content in green tea water during the steeping process. The experimental findings indicate that GTPs are the primary influencing factor of the output current signal. Furthermore, there is an inverse relationship between the concentration of GTPs in green tea water and the output current signal value. As the concentration increases, the current signal values decrease. A comparison of the polyphenol content in green tea originating from five different regions when steeped in boiling water revealed that the Nanjian tea water had the highest concentration of GTPs. According to the experimental results, the self-powered sensor could identify that the lowest concentration of tea polyphenols in green tea water was 27.84 μg mL^{-1}. The short-circuit current response time of the self-powered sensor reached 2 ms when the concentration of the tea polyphenol solution was at 0.05 mg mL^{-1}, while the open-circuit voltage response time reached 4 ms. In the experiment, the current sensitivity of the self-powered sensor reached −40.12 μA mg mL^{-1}, and the voltage sensitivity reached −0.195 V μg mL^{-1}. Additionally, this self-powered droplet sensor holds promising prospects for various applications in the field of solution component concentration detection and beyond.

Methods

Preparation of solutions

Preparation of green tea water at room temperature with different solid–liquid ratios. 1 g of Biluochun green tea was weighed and ground into powder. Then, 10, 20, 30, 40, 50, 60, 70, and 80 mg was taken, respectively, and placed in glass cups. 50 mL of room-temperature ultra-pure water was added to each cup and the tea powder was allowed to steep for 10 minutes. Afterward, the solutions were filtered to remove insoluble impurities and the resulting solutions were used for electrical signal testing. The same procedure was followed for the other four types of room-temperature green teas (Chuluoqing, Longjing, Zhangjiajie, and Nanjian).

Preparation of the GTP solution at room temperature. 25 mg, 50 mg, 75 mg, 100 mg, 125 mg, 150 mg, 175 mg, and 200 mg of tea polyphenol powders were weighed separately. Each precisely measured amount was dissolved in 50 mL of ultrapure water by gently stirring until complete dissolution was achieved. Employing the identical procedure, solutions with varying concentrations of pectin and L-theanine were generated.

Preparation of green tea water with different dilution ratios. 1 g of Biluochun green tea was weighed and ground. Then, 200 mg of the ground tea was taken and placed in a glass. 50 mL of boiling ultra-pure water was added to the glass and the tea soaked for 10 minutes. Afterward, the mixture was filtered and 5 mL, 2.5 mL, and 1 mL samples of the filtered tea water were collected separately. Each sample was transferred into a 50 mL flask and the volume adjusted to a fixed amount. The tea water was diluted to ratios of 10, 20, and 50 times, respectively, by adding the appropriate amount of additional water. The preparation method for the other four types of hot green tea water (Chuluoqing, Longjing, Zhangjiajie, and Nanjian) was the same as described above. In total, there were 15 cups of green tea water.

Preparation of fluorescein solution (10 wt%). 20 mL of fluorescein reagent was transferred to a 200 mL volumetric flask, diluted with ultra-pure water to the mark, and mixed well.

Preparation of Na$_2$CO$_3$ solution (7.5 wt%). 37.50 ± 0.01 g of Na$_2$CO$_3$ was weighed and dissolved in an appropriate amount of ultra-pure water. The resulting solution was transferred to a 500 mL volumetric flask and diluted up to the mark. The flask was shaken well to achieve proper mixing.

Preparation of gallic acid standard solution. 0.110 g ± 0.001 g of gallic acid was weighed and dissolved in a 100 mL volumetric flask, filling it up to the mark with solvent. It was shaken well to ensure thorough mixing. Using a pipette, 1.0 mL, 2.0 mL, 3.0 mL, 4.0 mL, and 5.0 mL samples of the gallic acid standard stock solution were transferred into separate 100 mL volumetric flasks. Each flask was filled to the mark with ultra-pure water and shaken well to prepare gallic acid working solutions.

Preparation of a self-powered droplet sensor. A 5 cm × 5 cm × 30 μm section of conductive copper foil tape was tightly adhered to an acrylic substrate. Then a piece of 5 cm × 5 cm ×

30 μm fluorinated ethylene propylene (FEP) tape was closely applied to cover the copper foil bottom electrode, preventing contact between droplets and the bottom electrode. Finally, conductive aluminum foil tape with dimensions of 1 cm × 2 mm × 30 μm was affixed.

Measurements

Measurements of the output current and output voltage values. The glass of filtered green tea water was placed on a homemade rack. A medical infusion tube was used to siphon the green tea water to a height of 20 cm above the device. The valve switching was controlled to regulate the frequency of green tea water drops, aiming for approximately 1 Hz. The electrical signals produced by the self-powered droplet sensor were measured using a Keithley 6514 electrometer controlled by a computer.

Measuring of absorption values of GTPs. 1.0 mL of green tea water at different dilution ratios and 1.0 mL of ultra-pure water (as a blank control) were added into separate graduated test tubes. 5.0 mL of fluorescein solution was added to each test tube and mixed well. After 3 to 8 minutes, 4.0 mL of 7.5% Na_2CO_3 solution was added to each tube and the volume was brought up to the mark with water, ensuring thorough mixing. It was left to stand at room temperature for 60 minutes. The absorbance was measured using a UV-Vis-NIR spectrophotometer at 765 nm using a 10 mm cuvette.

Measuring the absorption values of the gallic acid working solution. 1.0 mL of the gallic acid working solution and 1.0 mL of ultra-pure water (as a blank control) were added into separate graduated test tubes. 5.0 mL of fluorescein solution was added to each test tube and mixed well. After 3 to 8 minutes, 4.0 mL of 7.5% Na_2CO_3 solution was added to each tube and the volume was brought up to the mark with water, ensuring thorough mixing. It was left to stand at room temperature for 60 minutes. The absorbance was measured using a UV-Vis-NIR spectrophotometer at 765 nm using a 10 mm cuvette. Based on the absorbance of the gallic acid working solution and the known concentrations of gallic acid in each working solution, a standard curve was plotted. The slope (k) of the gallic acid standard curve was calculated.

Data availability

The data that support the findings of this study are available from the corresponding author [Guochen Lin, 18400213@muc.edu.cn], upon reasonable request.

Conflicts of interest

The authors declare no conflict of interest.

Acknowledgements

References

1 F. R. Fan, Z. Q. Tian and Z. L. Wang, *Nano Energy*, 2012, **1**, 328–334.
2 H. Wang, J. Cheng, Z. Wang, L. Ji and Z. L. Wang, *Sci. Bull.*, 2021, **66**, 490–511.
3 Y. Zeng, H. Xiang, N. Zheng, X. Cao, N. Wang and Z. L. Wang, *Nano Energy*, 2022, **91**, 106601.
4 S. Wang, J. Gao, F. Lu, F. Wang, Z. You, M. Huang, W. Fang, X. Liu, Y. Li and Y. Liu, *Nano Energy*, 2023, **108**, 108230.
5 D. Tan, J. Zhou, K. Wang, C. Zhang, Z. Li and D. Xu, *Nano Energy*, 2023, **109**, 108315.
6 J. Bae, J. Song, W. Jeong, K. R. Nandanapalli, N. Son, N. A. B. Zulkifli, G. Gwon, M. Kim, S. Yoo, H. Lee, H. Choi, S. Lee, H. Cheng, C. Kim, K. I. Jang and S. Lee, *Nano Energy*, 2022, **97**, 107223.
7 F. Gao, Z. Zhang, Q. Liao, G. Zhang, Z. Kang, X. Zhao, X. Xun, Z. Zhao, L. Xu, L. Xue and Y. Zhang, *Adv. Energy Mater.*, 2019, **9**, 1901881.
8 Y. Yang, L. Zheng, J. Wen, F. Xing, H. Liu, Y. Shang, Z. L. Wang and B. Chen, *Adv. Funct. Mater.*, 2023, **33**, 2304366.
9 C. Zhang, L. He, L. Zhou, O. Yang, W. Yuan, X. Wei, Y. Liu, L. Lu, J. Wang and Z. L. Wang, *Joule*, 2021, **5**, 1613–1623.
10 J. Cao, X. Fu, H. Zhu, Z. Qu, Y. Qi, Z. Zhang, Z. Zhang, G. Cheng, C. Zhang and J. Ding, *Small Methods*, 2022, **6**, 2200588.
11 W. Qiao, L. Zhou, Z. Zhao, P. Yang, D. Liu, X. Liu, J. Liu, D. Liu, Z. L. Wang and J. Wang, *Nano-Micro Lett.*, 2023, **15**, 218.
12 Y. Song, N. Wang, Y. Wang, R. Zhang, H. Olin and Y. Yang, *Adv. Energy Mater.*, 2020, **10**, 2002756.
13 Z.-H. Lin, G. Cheng, L. Lin, S. Lee and Z. L. Wang, *Angew. Chem., Int. Ed.*, 2013, **52**, 12545–12549.
14 Z. L. Wang and A. C. Wang, *Mater. Today*, 2019, **30**, 34–51.
15 D. L. Vu, C. D. Le, C. P. Vo and K. K. Ahn, *Composites, Part B*, 2021, **223**, 109135.
16 Y. Zeng, Y. Luo, Y. Lu and X. Cao, *Nano Energy*, 2022, **98**, 107316.
17 Q. Wu, L. Zhang, W. Wang, H. Xu, J. Cheng, X. Wu, Y. Liu, X. Zhang and D. Wang, *Nano Energy*, 2024, **123**, 109391.
18 X. Guo, F. Li, Z. Xi, J. Hong, Y. Wang, Z. Qian, H. Yu, C. Zhu, H. Du, J. Si, H. Wang and M. Xu, *ACS Appl. Electron. Mater.*, 2024, **6**, 376–385.
19 P. Wu, P. Yang, Z. Liu, G. Huang, X. Tao, S. Qin, X. Dong, L. Zheng, H. Li, X. Chen and Z. L. Wang, *Adv. Energy Mater.*, 2024, **14**, 2303912.
20 J. Zhang, S. Lin, M. Zheng and Z. L. Wang, *ACS Nano*, 2021, **15**, 14830–14837.

21 J. Zhang, X. Wang, L. Zhang, S. Lin, S. Ciampi and Z. L. Wang, *J. Am. Chem. Soc.*, 2024, **146**, 6125–6133.

22 C. Wang, P. Wang, J. Li, Y. Sun, W. Lu, D. Zhang, Y. Wan and S. Ai, *Adv. Funct. Mater.*, 2023, **33**, 2302524.

23 X. Li, L. Zhang, Y. Feng, Y. Zheng, Z. Wu, X. Zhang, N. Wang, D. Wang and F. Zhou, *Adv. Funct. Mater.*, 2021, **31**, 2010220.

24 S. Chatterjee, S. Saha, S. R. Barman, I. Khan, Y.-P. Pao, S. Lee, D. Choi and Z.-H. Lin, *Nano Energy*, 2020, **77**, 105093.

25 X. Wei, B. Wang, X. Cao, H. Zhou, Z. Wu and Z. L. Wang, *Nat. Food*, 2023, **4**, 721–732.

26 M.-F. Sun, C.-L. Jiang, Y.-S. Kong, J.-L. Luo, P. Yin and G.-Y. Guo, *Foods*, 2022, **11**(10), 1425.

27 L. Xing, H. Zhang, R. Qi, R. Tsao and Y. Mine, *J. Agric. Food Chem.*, 2019, **67**, 1029–1043.

28 M. A. Hidayat, F. Jannah and B. Kuswandi, *Agric. Agric. Sci. Procedia*, 2016, **9**, 424–430.

29 Z. Guo, A. O. Barimah, L. Yin, Q. Chen, J. Shi, H. R. El-Seedi and X. Zou, *Food Chem.*, 2021, **353**, 129372.

30 M. K. Al-Shwaiyat, D. Tatyana, Y. Miekh and A. Vishnikin, *Chem. Chem. Technol.*, 2018, **12**, 135–142.

31 C. S. Martin, M. D. Maximino, M. S. Pereira and P. Alessio, *IEEE Sens. J.*, 2019, **19**, 10686–10692.

32 W. Xu, H. Zheng, Y. Liu, X. Zhou, C. Zhang, Y. Song, X. Deng, M. Leung, Z. Yang, R. X. Xu, Z. L. Wang, X. C. Zeng and Z. Wang, *Nature*, 2020, **578**, 392–396.

33 W. Xu, X. Li, J. Brugger and X. Liu, *Nano Energy*, 2022, **98**, 107166.

34 Q. Zhou, B. Wang, A. Gao, W. Xu, K. Zhou, J. Pan, G. Meng, C. Pan and F. Xia, *Adv. Funct. Mater.*, 2022, **32**, 2209100.